J. Fluid Mech. (1975), *vol.* 67, *part* 3, *pp.* 497–511
Printed in Great Britain

Rectangular resonators on infinite and semi-infinite channels

By V. T. BUCHWALD AND N. V. WILLIAMS†
School of Mathematics, University of New South Wales, Kensington

(Received 18 October 1973 and in revised form 1 May 1974)

The surface elevations in a strip $0 < y < b$ and in a rectangle $-d < y < 0$, $|x| < a$ are expressed as a Fourier integral and Fourier series respectively. Using a Galerkin technique to match boundary conditions, the solution to the general problem of the response of a rectangular resonator to inviscid shallow-water waves in infinite and semi-infinite channels is obtained.

Theoretical results are compared with laboratory experiments of James (1970, 1971*a*, *b*). Agreement is generally very good, except that the inviscid and linear theory does not predict the observed large energy losses in the resonator at resonance.

The theory is also applied to a geometry corresponding to the Gulf of Carpentaria, and the calculated response of the Gulf to semi-diurnal tides gives a zero response at Kuramba, in agreement with observations. The full response of the Gulf is calculated in subsequent work (Williams 1974) which takes the effects of the earth's rotation into account.

1. Introduction

The initial intention of this investigation was to obtain a first approximation to the tidal problem in the Gulf of Carpentaria. Assuming a simplified geometry, and that the effects of friction and the earth's rotation are comparatively small, the tidal problem was reduced to the determination of the response of a rectangular sea to a tidal input from a canal whose width is of the same order as the dimensions of the sea (see figure 1*b*). During the course of the investigation James (1970) published the results of laboratory experiments on the effects of resonators on the transmission of water waves in rectangular canals. The intention of this paper, then, is to obtain a theoretical model for the response of a rectangular resonator in either an open canal or an L-shaped canal, as in figures 1(*a*) and (*b*). The results of this general investigation can then be applied to both the above experimental situations.

The mathematical methods used are fairly standard (for instance, Miles 1947; Miles & Munk 1961; Miles & Gilbert 1968), although there are some analytic and computational points which are special to this case. In addition, rather than using the variational formulation adopted by previous authors, we shall use the

† Present address: Aeronautical Research Laboratories, Fisherman's Bend, Victoria 3207.

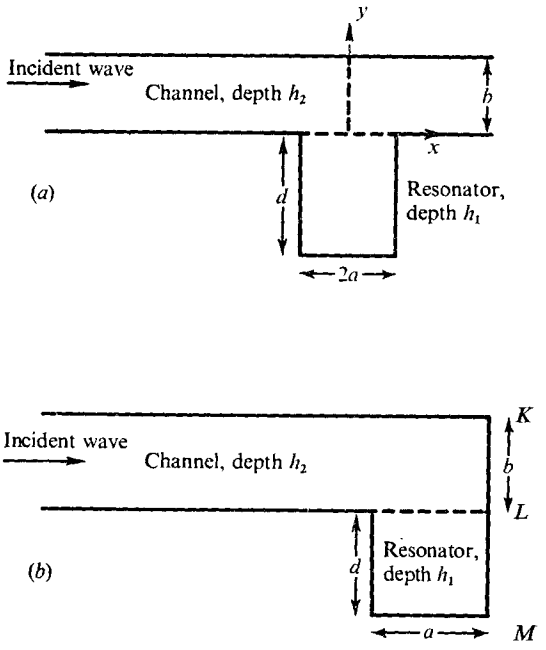

FIGURE 1. Plan of resonator with (*a*) an infinite channel and (*b*) a semi-infinite channel.

somewhat simpler Galerkin technique for solving the integral equations obtained, the accuracy of the solution being tested in each case by consideration of the size of the actual discrepancies in the quantities being matched approximately at the boundaries.

In order to illustrate some of the features of wave propagation in a canal and the response of a resonator, we shall first consider in § 3 the problem of a narrow resonator, and its effect on the transmission of waves along the canal. Some of the general results obtained in this simpler case illustrate certain of the physical properties which will be obtained later by numerical computation. Miles (1947) has considered somewhat similar problems for narrow wave guides, but the methods used in this paper are useful in a greater variety of situations. The general theory of wide resonators is given in § 4.

In § 5 numerical results are obtained and are found to be in excellent agreement with the experimental results of James (1971*a*, *b*), except that there seems to be a large loss of energy near resonance in the laboratory experiments, perhaps due to nonlinear effects at resonance. Finally, in § 6 some preliminary results on the tidal problem in the Gulf of Carpentaria are obtained. These show sufficiently good agreement with observations to warrant further refinement of the theoretical model.

2. Formulation of the basic equation

Assuming inviscid and linear shallow-water theory, the reduced equation for the surface displacement ζ_j is

$$\nabla^2\zeta_j + k_j^2\zeta_j = 0, \tag{2.1}$$

where the subscripts $j = 1$ and 2 refer to the resonator and channel region, respectively. The x and y axes are horizontal and in the directions illustrated in figure 1. The channel, of depth h_2, occupies the strip $0 < y < b$, and the resonator, of depth h_1, occupies the rectangle $-d < y < 0$, $|x| < a$, being connected to the channel across the boundary at $y = 0$, $|x| < a$.

In (2.1) it is assumed that ζ_j contains an implicit harmonic time factor

$$\exp(-i\omega' t),$$

where

$$\omega' = \omega + i\epsilon \tag{2.2}$$

and $\epsilon \ll \omega$. The purpose of the small imaginary part in ω' is to apply automatically a radiation condition to waves from the resonator, after which the limit $\epsilon \to 0$ gives the steady state. Then, in (2.1),

$$k_j^2 = \omega'^2/gh_j, \quad j = 1, 2. \tag{2.3}$$

The respective depth-averaged velocities $\mathbf{q}_j = (u_j, v_j)$ are given by

$$i\omega\mathbf{q}_j = g\nabla\zeta_j. \tag{2.4}$$

From (2.4) the boundary conditions are

$$\text{(i)}\ \partial\zeta_2/\partial y = 0 \quad \text{for} \quad \begin{cases} y = b, & \text{all } x, \qquad (2.5a) \\ y = 0, & |x| > a, \qquad (2.5b) \end{cases}$$

$$\text{(ii)}\ \partial\zeta_1/\partial y = 0 \quad \text{for} \quad y = -d, \quad |x| < a, \tag{2.6}$$

$$\text{(iii)}\ d\zeta_1/\partial x = 0 \quad \text{for} \quad 0 > y > -d, \quad x = \pm a, \tag{2.7}$$

while the continuity conditions across the resonator mouth are (Bartholomeuzs 1958)

$$\text{(iv)} \quad \left.\begin{aligned} \zeta_1 &= \zeta_2 \qquad (2.8a) \\ h_1\partial\zeta_1/\partial y &= h_2\partial\zeta_2/\partial y = f(x) \qquad (2.8b) \end{aligned}\right\} \quad \text{for} \quad y = 0, \quad |x| < a.$$

The symmetric case

Let us suppose first of all that ζ_1, ζ_2 and $f(x)$ are even functions of x. A general expression for ζ_1 is the Fourier expansion

$$\zeta_{1S} = \sum_{n=0}^{\infty} A_n \cos\mu_n x \cos p_n(y+d), \tag{2.9}$$

where $\mu_n = n\pi/a$, which satisfies the boundary conditions (2.6) and (2.7) and the differential equation (2.1) provided that

$$p_n = (k_1^2 - \mu_n^2)^{\frac{1}{2}}. \tag{2.10}$$

Moreover, if, as in (2.8b), $h_1 \partial\zeta_{1S}/\partial y = f(x)$ at $y = 0$, we have that

$$f(x) = \sum_{n=0}^{\infty} f_n \cos\mu_n x, \quad |x| < a, \tag{2.11}$$

where f_n and A_n are related by

$$A_n h_1 p_n \sin p_n d + f_n = 0. \tag{2.12}$$

Now suppose that in the channel

$$\zeta_2 = \zeta_{0S} + \zeta_{2S}, \tag{2.13}$$

where ζ_{0S} is the symmetric part of an incident disturbance which satisfies

$$\partial\zeta_{0S}/\partial y = 0 \quad \text{for} \quad y = 0, b, \quad \text{all } x, \tag{2.14}$$

while ζ_{2S} satisfies the conditions (2.5) and (2.8) and represents the waves radiating from the resonator. Then ζ_{2S} may be written as the Fourier integral

$$\zeta_{2S} = \int_0^{\infty} \phi(\lambda) \cosh\sigma(y-b) \cos\lambda x \, d\lambda. \tag{2.15}$$

This satisfies (2.1) and (2.5a) if

$$\sigma = (\lambda^2 - k_2^2)^{\frac{1}{2}}, \tag{2.16}$$

and (2.5b) and (2.8b) provided that

$$\begin{aligned} h_2\sigma \sinh\sigma b \, \phi(\lambda) &= -\frac{2}{\pi}\int_0^a f(x)\cos\lambda x \, dx \\ &= -\frac{2\lambda \sin a\lambda}{\pi} \sum_{n=0}^{\infty} \frac{(-1)^{n+1} f_n}{\mu_n^2 - \lambda^2}, \end{aligned} \tag{2.17}$$

by (2.11). Finally, (2.8a) is satisfied if

$$\zeta_{0S}(x, 0) + \zeta_{2S}(x, 0) = \zeta_{1S}(x, 0), \quad |x| < a, \tag{2.18}$$

where ζ_{0S} is a given symmetric function, and, in terms of the unknown f_n,

$$h_1\zeta_{1S}(x, 0) = -\sum_{n=0}^{\infty} (f_n/p_n) \cos\mu_n x \cot p_n d, \tag{2.19}$$

$$h_2\zeta_{2S}(x, 0) = -\frac{2}{\pi}\int_0^{\infty} \frac{\lambda \coth\sigma b}{\sigma} \sum_{n=0}^{\infty} \frac{(-1)^{n+1} f_n}{\mu_n^2 - \lambda^2} \cos\lambda x \sin a\lambda \, d\lambda. \tag{2.20}$$

The problem, then, is to determine the coefficients f_n so that (2.18) is satisfied.

The antisymmetric case

We now assume that ζ_{1A}, ζ_{2A} and $g(x)$ are odd functions. In this case

$$\zeta_{1A}(x, y) = \sum_{n=0}^{\infty} B_n \sin\mu_{n'} x \cos p_{n'}(y + d), \tag{2.21}$$

$$g(x) = \sum_{n=0}^{\infty} g_n \sin\mu_{n'} x, \tag{2.22}$$

where
$$p_{n'} = (k_1^2 - \mu_{n'}^2)^{\frac{1}{2}}, \quad \mu_{n'} = n'\pi/a, \quad n' = n + \tfrac{1}{2} \tag{2.23}$$

and
$$B_n h_1 p_{n'} \sin p_{n'} d + g_n = 0. \tag{2.24}$$

Again suppose that

$$\zeta_2 = \zeta_{0A} + \zeta_{2A}, \tag{2.25}$$

where ζ_{0A} is the antisymmetric part of some incident disturbance and

$$\zeta_{2A} = \int_0^\infty \psi(\lambda) \cosh \sigma(y-b) \sin \lambda x \, d\lambda, \tag{2.26}$$

where σ is given by (2.16). Inverting the sine transforms for $y = 0$ gives

$$h_2 \sigma \sinh \sigma b \, \psi(\lambda) = -\frac{2\lambda \cos a\lambda}{\pi} \sum_{n=0}^{\infty} \frac{(-1)^n g_n}{\mu_{n'}^2 - \lambda^2}. \tag{2.27}$$

Equating surface elevations at the mouth of the resonator again results in an equation of the form (2.18), with, in this case,

$$h_1 \zeta_{1A}(x, 0) = -\sum_{n=0}^{\infty} (g_n / p_{n'}) \sin \mu_{n'} x \cot p_{n'} d \tag{2.28}$$

and

$$h_2 \zeta_{2A}(x, 0) = -\frac{2}{\pi} \int_0^\infty \frac{\lambda \coth \sigma b \sin \lambda x \cos a\lambda}{\sigma} \sum_{n=0}^{\infty} \frac{(-1)^n g_n}{\mu_{n'}^2 - \lambda^2} \, d\lambda. \tag{2.29}$$

3. The narrow resonator

In order to illustrate some of the features of the response of the resonator we first consider the case in which $2k_2 a \ll 1$, that is the width of the resonator is much less than $(2\pi)^{-1} \times$ (length of the incoming wave).

We assume that without the resonator there is a wave in the channel represented by

$$\zeta_2^* = Z \exp[i(k_2 x - \omega' t)], \tag{3.1}$$

so that as a first approximation

$$\zeta_{0S} = Z \tag{3.2}$$

in (2.18), and $\zeta_{0A} = 0$ in the corresponding equation in the antisymmetric case. We also assume that the velocity v is uniform across the mouth of the resonator, so that the series in (2.9) is approximated by its first term and $f_n = 0$ for all $n \geqslant 1$ in (2.11), (2.17), (2.19) and (2.20). We now satisfy (2.18) on the average, i.e. by integrating this equation from $-a$ to a, with the result that

$$A_0 = -f_0 / h_1 k_1 \sin k_1 d = Z/\Gamma, \tag{3.3}$$

where

$$\Gamma = \cos k_1 d - \Lambda k_1 \sin k_1 d \tag{3.4}$$

and

$$\Lambda = \alpha + i\beta = \frac{2\tau}{\pi a} \int_0^\infty \sigma^{-1} \coth \sigma b \left(\frac{\sin a\lambda}{\lambda} \right)^2 d\lambda, \tag{3.5}$$

with

$$\tau = h_1 / h_2.$$

The integral in (3.5) can be extended over the whole of the real line and then evaluated by standard methods of contour integration. The poles of the integrand are at $\lambda = 0$, at $\lambda = \pm \lambda_n$, $0 \leqslant n \leqslant N$, and at $\lambda = \pm i\rho_n$, $n \geqslant N+1$, where

$$\lambda_n^2 = k_2^2 - n^2\pi^2/b^2, \quad \rho_n^2 = n^2\pi^2/b^2 - k_2^2, \tag{3.6}$$

and N is such that $n\pi/b < \mathscr{R}(k_2)$ for $n \leqslant N$ while $n\pi/b > \mathscr{R}(k_2)$ for $n \geqslant N+1$. *Remembering that k_2 contains a small positive imaginary part $O(\epsilon)$, we obtain* the result

$$\alpha = \frac{\tau}{ab}\sum_{n=0}^{N}\epsilon_n\frac{\sin 2a\lambda_n}{\lambda_n^3}+\frac{\tau}{ab}\sum_{n=N+1}^{\infty}\frac{\exp(-2a\rho_n)-1}{\rho_n^3}-\frac{\tau\cot bk_2}{k_2}, \tag{3.7}$$

$$\beta = \frac{\tau}{ab}\sum_{n=0}^{N}\epsilon_n(1-\cos 2a\lambda_n)/\lambda_n^3, \tag{3.8}$$

where $\epsilon_0 = \frac{1}{2}$ and $\epsilon_n = 1$ for all other n. Note that both α and β are $O(a)$ as $a \to 0$. This is obvious in the case of β, but the well-known series

$$b\cot bk_2 = \frac{1}{k_2}+2\sum_{n=1}^{\infty}\frac{k_2}{k_2^2-n^2\pi^2/b^2}$$

needs to be used to prove the result for α. The greatest amplitude of ζ_1 occurs at $y = -d$, when $|\zeta_1| = |A_0|$, and this is a maximum when $|\Gamma|$ is a minimum. Assuming that ϵ in (2.2) is vanishingly small and that $k_1 a$ is small enough so that terms $O(k_1^2a^2)$ may be neglected, resonance for fixed ω' and varying d occurs when $d = d_m$, where

$$k_1 d_m = \tfrac{1}{2}\pi - \alpha k_1 + m\pi + O(a^2k_1^2), \quad m = 0, 1, 2, \ldots, \tag{3.9}$$

and the resonant amplitude $A_0^{(m)}$ is given by

$$(-1)^m A_0^{(m)} = iZ/\beta k_1 + O(ak_1). \tag{3.10}$$

On the other hand, if d is fixed and ω' is variable, then at resonance

$$\omega'_m = (gh_1)^{\frac{1}{2}}k_1^{(m)},$$

where

$$k_1^{(m)}d = (m+\tfrac{1}{2})\pi(1-\alpha/d), \tag{3.11}$$

and

$$(-1)^m A_0^{(m)} = iZd/(m+\tfrac{1}{2})\pi\beta + O(1) \tag{3.12}$$

as $a/d \to 0$. In particular, when $N = 0$, then, for small a, (3.8) simplifies to

$$\beta = (\tau a/k_2 b)(1+O(a^2k_2^2)),$$

so that, noting that $k_2/k_1 = \tau^{\frac{1}{2}}$, it follows from (3.10) that the resonant amplitude is given by

$$(-1)^m A_0^{(m)} = iZb/a\tau^{\frac{1}{2}},$$

which is independent of the resonant frequency and of m, in all cases where the frequency satisfies the inequality

$$\omega^2 < gh_2\pi^2b^2,$$

so that $N = 0$. Note that the result in (3.9) is the first-order correction to the quarter-wavelength resonance assumed by Valembois (1953) for a narrow resonator.

We are also interested in the amplitudes of the reflected and transmitted waves in the channel. From (2.15), (2.17) and (3.3),

$$\zeta_{2S}(x,y) = -\frac{f_0}{\pi h_2}\int_{-\infty}^{\infty}\frac{\sin a\lambda\cosh\sigma(y-b)}{\lambda\sigma\sinh\sigma b}e^{i\lambda x}d\lambda. \tag{3.13}$$

The integral is evaluated by completing a circuit with a large semicircular contour in the upper half-plane if $x > a$ and in the lower half-plane if $x < -a$, with the result that

$$\zeta_2 = \frac{2ik_1\tau Z}{b(\cot k_1 d - \Lambda k_1)}\left(\sum_{n=0}^{N}\epsilon_n \frac{\sin a\lambda_n \cos[n\pi y/b]}{\lambda_n^2}\exp(i\lambda_n|x|)\right.$$
$$\left. - i\sum_{n=N+1}^{\infty}\frac{\sinh a\rho_n \cos[n\pi y/b]}{\rho_n^2}\exp(-\rho_n|x|)\right), \quad (3.14)$$

where Λ, λ_n and ρ_n are defined in (3.5) and (3.6). We now see that the poles at $\lambda = \theta_n$, near the real axis, correspond to the $N+1$ real modes of propagation in the channel, while the poles at $\lambda = i\rho_n$ give modes which decay as $|x| \to \infty$.

In particular, if $N = 0$, there is only one possible mode of propagation in the channel. At resonance ω' and $k_1 d$ are given by (3.9), and then, if ak_2 is sufficiently small to assume that $\sin ak_2 \approx ak_2$,

$$\zeta_{2S} = -Z\exp(ik_2|x|) + \text{decaying modes}, \quad |x| > a. \quad (3.15)$$

Comparing this with (3.1), we recover the result that at resonance the incident wave is completely reflected with a change of phase, and there is no transmitted wave. In the general case we have that at resonance for $|x| > a$

$$\left\{\sum_{n=0}^{N}\epsilon_n\lambda_n^{-1}\right\}\zeta_{2S} = -Z\sum_{n=0}^{N}\epsilon_n\lambda_n^{-1}\cos(n\pi y/b)\exp(i\lambda_n|x|) + \text{decaying modes}.$$

Note that if $k_2 = n\pi/b + \delta$, where δ is small, then ω' is near the cut-off frequency of the nth mode, and to within $O(\delta)$, the whole of the energy is converted into the nth mode.

The analysis in this section has been carried out for an infinite channel as in figure 1 (*a*). However, it also applies to a semi-infinite resonator, as in figure 1 (*b*), by simply assuming that instead of (3.1)

$$\zeta_0^* = Z\cos k_2 x\, e^{-i\omega' t}.$$

4. The theory of wide resonators

In this section we drop the assumption of the previous section that $ak_2 \ll 1$, and adopt a Galerkin technique to determine the coefficients f_n in (2.18) and the coefficients g_n in the equivalent to (2.18) in the antisymmetric case.

Assume first that $\zeta_0(x, 0)$ is symmetric about $x = 0$, multiply (2.18) by $\cos\mu_m x$ (where $\mu_m = n\pi/a$) and integrate with respect to x over the interval $[-a, a]$ to obtain the sequence of equations

$$\frac{\epsilon_m a\cot p_m d}{h_1 p_m}f_m - \frac{4}{\pi h_2}\sum_{n=0}^{\infty}(-1)^{m+n}I_{mn}f_n = K_m, \quad (4.1)$$

for $m = 0, 1, 2, \ldots$, etc., where

$$K_m = -\int_{-a}^{a}\zeta_0(x, 0)\cos\mu_m x\, dx \quad (4.2)$$

and

$$I_{mn} = \int_0^{\infty}\frac{\lambda^2\coth\sigma b\sin^2\lambda a}{\sigma(\lambda^2-\mu_m^2)(\lambda^2-\mu_n^2)}d\lambda. \quad (4.3)$$

Note that I_{00} is the integral in (3.5) and that I_{mn} may be similarly evaluated in series form by contour integration. Note also that for an incident plane wave as in (3.1)

$$K_m = 2k_2 Z \sin ak_2(-1)^m/(k_2^2 - \mu_m^2). \tag{4.4}$$

The sequence of equations (4.1) is solved approximately by terminating the series at $m = M-1$, whence estimates for f_m for $m < M$ are obtained. Approximate forms for $\zeta_{1S}(x, y)$ are now obtained from (2.9) and (2.12), and for $\zeta_{2S}(x, y)$ from (2.15) and (2.17). The extent to which the relation (2.18) is satisfied with increasing M will give a test of the efficiency of the method, as will the rate of convergence of the f_m, with m fixed, for increasing M. Details of the computational procedure may be found in Williams (1973), as may details of the antisymmetric case, and for the L-shaped resonator at the end of a semi-infinite channel.

5. Infinite channels

The theoretical and numerical results in this section are intended as complementary to the laboratory experiments of James (1970, 1971*a*, *b*). The theoretical results give a very accurate prediction of the geometry and frequencies for which resonance or anti-resonance takes place, as well as a good prediction of the response of the system when not in resonance. However, at resonance it would appear that in the laboratory situation at least half the energy of the incident wave is lost within the immediate neighbourhood of the resonator.

In order to establish the accuracy of the theory, we shall first consider in detail a particular case, not near resonance. It will be seen that in this case the Galerkin procedure converges rapidly, and for $M = 10$ there is excellent agreement between the displacements calculated at the boundary between the channel and resonator. We shall next consider cases which can be compared directly with the experimental results, and the section will then be concluded with some calculations for geometries for which experimental results are not available.

A detailed example

Assume that $h_1 = h_2$, so that $k_1 = k_2 = k$ and the wavelength of the incident wave $W = 2\pi/k$. The actual numerical values taken in this example are

$$2a/W = 0{\cdot}34, \quad b/W = 0{\cdot}385, \quad d/W = 0{\cdot}20. \tag{5.1}$$

Tables 1 and 2 give the computed values of the f_n and g_n, respectively, for $M = 2, 4, 6, 8$ and 10. Comparison of computed displacements on either side of the junction line at $|x| \leqslant a$, $y = 0$ shows very good agreement for $M = 10$, except for some discrepancies near the corners at $x = \pm a$.

The theory in this paper is for shallow water, and is valid if $h/W \ll 1$. On the other hand, the parameters in James's experiments do not satisfy this criterion. Nevertheless, if we assume that $h_1 = h_2 = h$, then the two theories are entirely analogous in the sense that all geometrical results are identical. The only difference is that, if $\bar{\omega}$ is the frequency in the laboratory and ω the frequency in the shallow-water theory, then

$$(\bar{\omega}/\omega)^2 = (W/2\pi h)\tanh(2\pi h/W).$$

Assuming, then, a uniform depth h, computed and observed results can be compared directly.

	$M = 2$	$M = 4$	$M = 6$	$M = 8$	$M = 10$
f_0	$1{\cdot}469 - 1{\cdot}228i$	$1{\cdot}478 - 1{\cdot}245i$	$1{\cdot}480 - 1{\cdot}250i$	$1{\cdot}481 - 1{\cdot}252i$	$1{\cdot}481 - 1{\cdot}253i$
f_1	$-0{\cdot}163 + 0{\cdot}136i$	$-0{\cdot}170 + 0{\cdot}143i$	$-0{\cdot}173 + 0{\cdot}146i$	$-0{\cdot}174 + 0{\cdot}147i$	$-0{\cdot}175 + 0{\cdot}148i$
f_2	—	$0{\cdot}148 - 0{\cdot}125i$	$0{\cdot}151 - 0{\cdot}128i$	$0{\cdot}153 - 0{\cdot}129i$	$0{\cdot}154 - 0{\cdot}130i$
f_3	—	$-0{\cdot}124 + 0{\cdot}104i$	$-0{\cdot}127 + 0{\cdot}107i$	$-0{\cdot}128 + 0{\cdot}109i$	$-0{\cdot}130 + 0{\cdot}110i$
f_4	—	—	$0{\cdot}110 - 0{\cdot}093i$	$0{\cdot}112 - 0{\cdot}094i$	$0{\cdot}113 - 0{\cdot}095i$
f_5	—	—	$-0{\cdot}098 + 0{\cdot}082i$	$-0{\cdot}099 + 0{\cdot}084i$	$-0{\cdot}101 + 0{\cdot}085i$
f_6	—	—	—	$0{\cdot}090 - 0{\cdot}076i$	$0{\cdot}092 - 0{\cdot}78i$
f_7	—	—	—	$-0{\cdot}083 + 0{\cdot}070i$	$-0{\cdot}085 + 0{\cdot}072i$
f_8	—	—	—	—	$0{\cdot}080 - 0{\cdot}068i$
f_9	—	—	—	—	$-0{\cdot}075 \pm 0{\cdot}063i$

TABLE 1. Values of f_n for various M

	$M = 2$	$M = 4$	$M = 6$	$M = 8$	$M = 10$
g_0	$0{\cdot}044 + 0{\cdot}517i$	$0{\cdot}045 + 0{\cdot}520i$	$0{\cdot}045 + 0{\cdot}521i$	$0{\cdot}045 + 0{\cdot}521i$	$0{\cdot}045 + 0{\cdot}521i$
g_1	$-0{\cdot}015 - 0{\cdot}176i$	$-0{\cdot}016 - 0{\cdot}180i$	$-0{\cdot}016 - 0{\cdot}182i$	$-0{\cdot}016 - 0{\cdot}182i$	$-0{\cdot}016 - 0{\cdot}183i$
g_2	—	$0{\cdot}010 + 0{\cdot}120i$	$0{\cdot}011 + 0{\cdot}122i$	$0{\cdot}011 + 0{\cdot}123i$	$0{\cdot}011 + 0{\cdot}123i$
g_3	—	$-0{\cdot}008 - 0{\cdot}093i$	$-0{\cdot}008 - 0{\cdot}095i$	$-0{\cdot}008 - 0{\cdot}096i$	$-0{\cdot}008 - 0{\cdot}096i$
g_4	—	—	$0{\cdot}007 + 0{\cdot}079i$	$-0{\cdot}007 + 0{\cdot}080i$	$0{\cdot}007 + 0{\cdot}081i$
g_5	—	—	$-0{\cdot}006 - 0{\cdot}068i$	$-0{\cdot}006 - 0{\cdot}069i$	$-0{\cdot}006 - 0{\cdot}070i$
g_6	—	—	—	$0{\cdot}005 + 0{\cdot}062i$	$0{\cdot}005 + 0{\cdot}063i$
g_7	—	—	—	$-0{\cdot}005 - 0{\cdot}056i$	$-0{\cdot}005 - 0{\cdot}057i$
g_8	—	—	—	—	$0{\cdot}005 + 0{\cdot}053i$
g_9	—	—	—	—	$-0{\cdot}004 - 0{\cdot}049i$

TABLE 2. Values of g_n for various M

Comparison with experiment

Assuming an incident wave of unit amplitude, figure 2 shows computed and experimental values of the amplitudes of the transmitted and reflected waves for varying d/W, with $2a/W = 0{\cdot}34$ and $b/W = 0{\cdot}385$. Noting that for this value of b/W only one mode is possible in the channel, the zero reflectivity at $d/W = 0{\cdot}155$ corresponds to actual resonance. The calculated values of the transmissivity agree very well with those of James (1970), while the reflectivity indicates general agreement, with the proviso that the large energy discrepancy near resonance cannot be explained by an inviscid and linear model. Figure 3 (*a*) shows the system response at resonance. Figure 3 (*b*) shows the response just below resonance, with $d/W = 0{\cdot}145$. Just above resonance, at say $d/W = 0{\cdot}165$, the sense of the amphidrome is changed from anticlockwise to clockwise.

For a wider resonator one would also expect resonances with nodal lines along the length of the resonator. For instance, if $2a/W = 0{\cdot}60$ and $b/W = 0{\cdot}385$ there are two resonances in the range considered, at $d/W = 0{\cdot}16$ and $0{\cdot}335$, illustrated by the zeros of the transmissivity in figure 4. The nodal line at resonance is illustrated in figure 5 (*a*) for $d/W = 0{\cdot}335$. The response at the lower resonance $d/W = 0{\cdot}16$ is illustrated in figure 5 (*b*). It should be noticed that the theoretical predictions of the surface elevation in figures 5 (*a*) and (*b*) are remarkably confirmed by the sketches of resonance made by James (1970, figures 2 and 3).

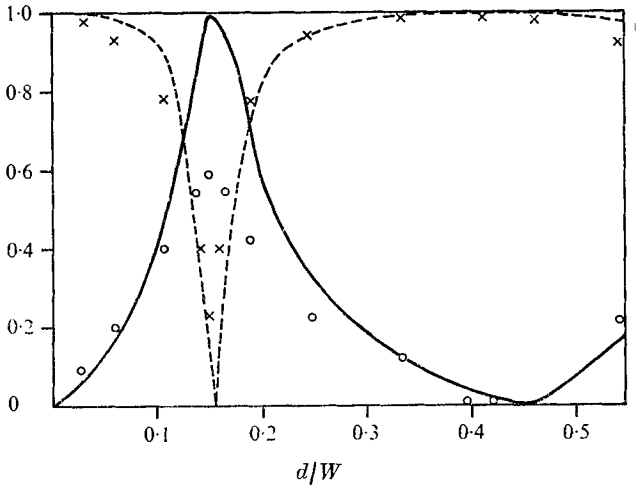

FIGURE 2. Transmitted and reflected wave amplitude for $b/W = 0{\cdot}385$, $2a/W = 0{\cdot}34$. Transmitted wave: ○, experimental points (James 1970); ——, theory. Reflected wave: ×, experimental points; – – – –, theory.

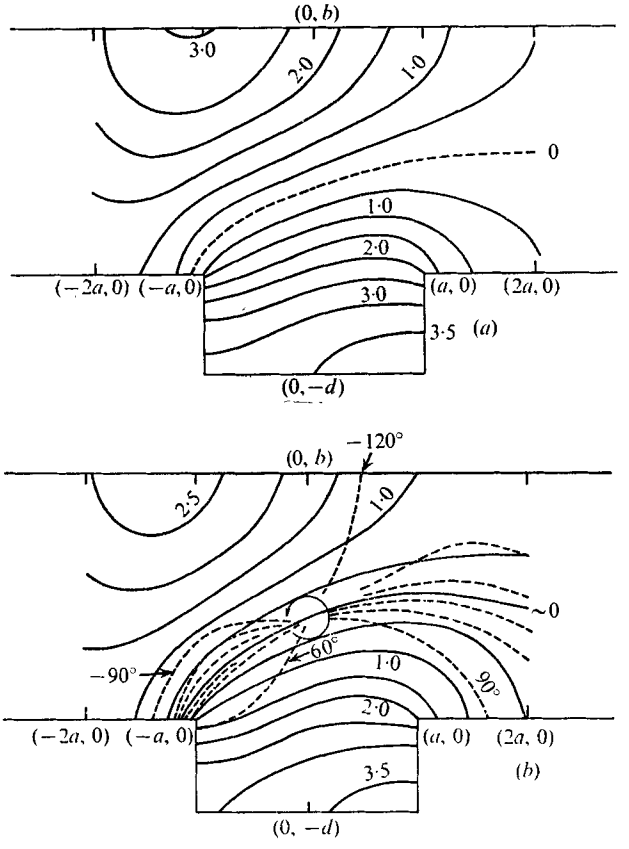

FIGURE 3. Response for $b/W = 0{\cdot}385$, $2a/W = 0{\cdot}34$. (*a*) At resonance; $d/W = 0{\cdot}155$. (*b*) Just below resonance; $d/W = 0{\cdot}145$.

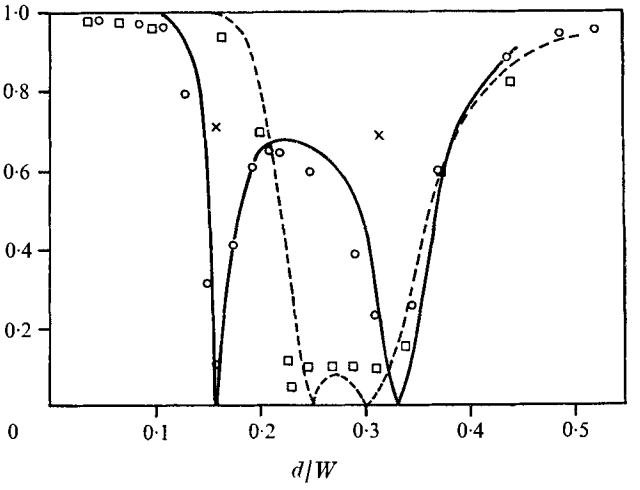

FIGURE 4. Wave amplitudes. (i) $2a/W = 0{\cdot}60$, $b/W = 0{\cdot}385$: ——, theoretical transmitted amplitude; ○, experimental transmissivity; ×, experimental reflected amplitude at resonance. (ii) $2a/W = 0{\cdot}616$, $b/W = 0{\cdot}308$: – – –, theoretical transmitted amplitude; □, experimental transmitted amplitude.

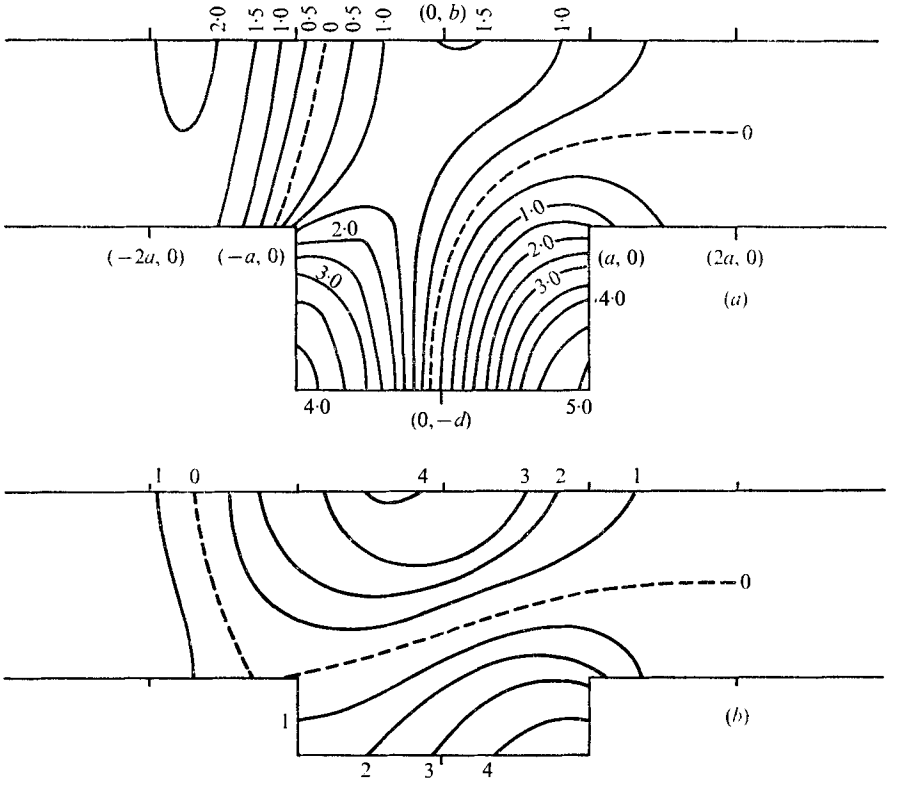

FIGURE 5. Co-amplitude lines at resonance for $2a/W = 0{\cdot}60$, $b/W = 0{\cdot}385$. (*a*) $d/W = 0{\cdot}335$ for an input wave of unit amplitude. (*b*) $d/W = 0{\cdot}16$.

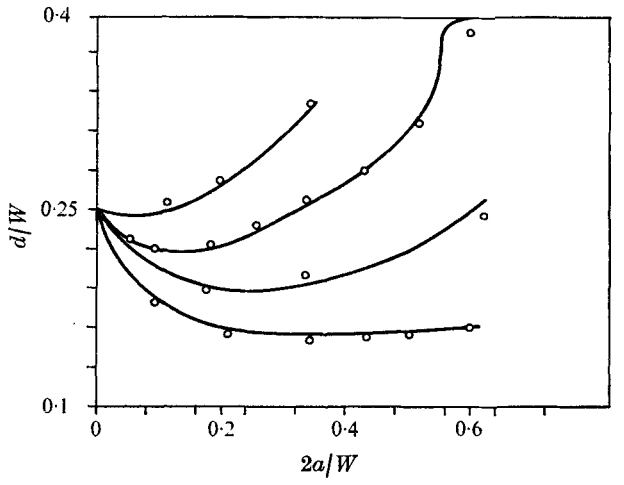

FIGURE 6. Comparison of theoretical determination of least-resonant length with experiments of James (1970) for different channel widths. Curves: 1, $b/W = 0{\cdot}086$; 2, $b/W = 0{\cdot}193$; 3, $b/W = 0{\cdot}308$; 4, $b/W = 0{\cdot}385$.

Figure 4 also gives the transmissivity for the case $2a/W = 0{\cdot}616$, $b/W = 0{\cdot}308$, when two resonances are very close together. Finally, in figure 6 the computed and observed values of the least-resonant lengths for different geometries are shown.

These and other (Williams 1973) results show that there is good agreement between the theory and experiment, particularly for the geometry at resonance, and for the transmissivity. There are energy losses near resonance which are probably due to nonlinear effects. Some evidence for this conjecture is given by James (1970), who observes that the increases in incident wave amplitude cause corresponding increases in energy losses.

Different depths

If $\tau < 1$ the wave speed in the resonator is reduced, and the general effect is as if the dimensions of the resonator were increased approximately in the ratio $\tau^{-\frac{1}{2}}$. The results of a typical set of calculations are given in figure 7, for $2a/W_2 = 0{\cdot}427$ and $b/W_2 = 0{\cdot}385$, where the resonant length d/W_2 is plotted against τ. The curves $S1$–$S3$ are the first three symmetric modes of resonance, in which the displacement is roughly uniform across the width of the resonator. The curves A_1 and A_2 are the first two antisymmetric modes.

The only experimental example is in James (1971*b*), where $\tau = 0{\cdot}14$, $W = 23{\cdot}4$ in., $h_1 = 1{\cdot}15$ in., $h_2 = 8{\cdot}2$ in. and the wave amplitude is 0·5 in. The experimental results are not really comparable with the theory for two reasons. First, the wave amplitude is not small compared with h_1, so that a linear theory is insufficient. Second, the wavelength is not sufficiently long, so that shallow-water theory does not hold in the channel, with the result that the boundary condition at the resonator mouth is suspect. Nevertheless, the experimental value of resonance at $d/W_2 = 0{\cdot}08$ agrees remarkably well with figure 7.

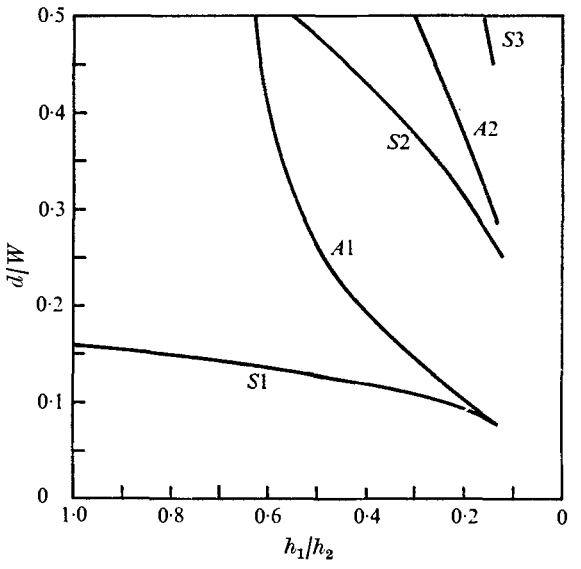

FIGURE 7. Resonant length for various values of τ, with $2a/W_2 = 0{\cdot}427$, $b/W = 0{\cdot}385$. $S1$, $S2$ and $S3$ are the symmetric modes, and $A1$ and $A2$ the antisymmetric modes.

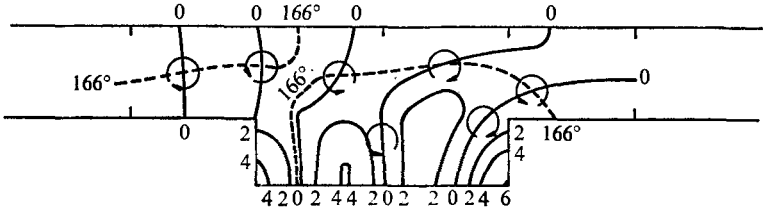

FIGURE 8. Response for a wide channel; $b/W = 0{\cdot}60$, $2a/W = 1{\cdot}62$, $d/W = 0{\cdot}4344$.

Wide channels

If $b/W > 0{\cdot}5$ there are at least two modes of propagation in the channel, and all possible propagating modes are present in the diffracted field. Moreover, minima in the total transmitted energy, or in any one mode, are not necessarily associated with resonance in the resonator. Williams (1973) has calculated the transmitted energies for a variety of geometries. As an illustration, figure 8 shows a resonance when $2a/W = 1{\cdot}62$, $b/W = 0{\cdot}60$ and $d/W = 0{\cdot}4344$. In this particular case the transmitted wave field is almost zero. What there is of the transmitted wave is mainly in the second mode, and there is a nodal line along the centre of the channel.

6. The closed channel

Although there are no experimental results available for a closed channel, it is possible to make some comparisons with geophysical examples. A simplified model of the Gulf of Carpentaria is as in figure 1 (*b*), with $a = 480\,\text{km}$, $d = 390\,\text{km}$, $b = 390\,\text{km}$, $h_1 = 54{\cdot}9\,\text{m}$ (30 fathoms) and $h_2 = 91{\cdot}5\,\text{m}$ (50 fathoms). The point

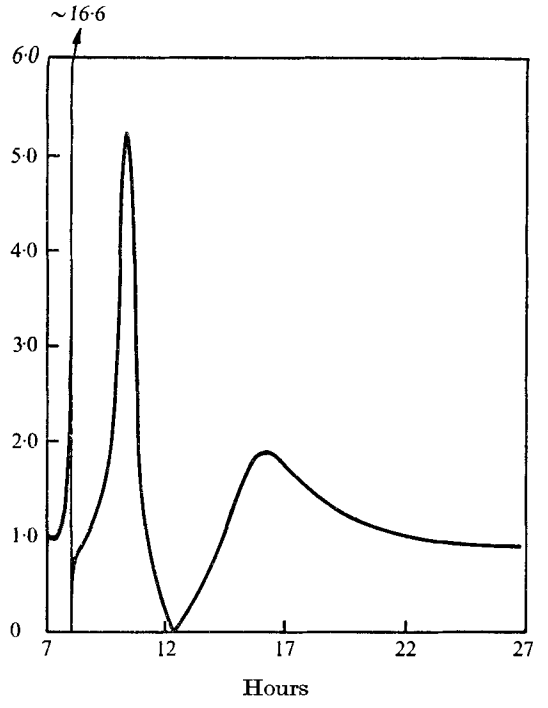

FIGURE 9. Theoretical response at Kuramba to an input of unit amplitude in the Arafura Sea.

K corresponds to tidal recording stations at Kuramba and at Bayley Island. Figure 9 gives the calculated response at K as a function of the period of an input of unit amplitude in the channel (Arafura Sea).

The most interesting feature is that the observed M_2 and S_2 tidal components at K are minute, and this is also shown in the calculated response at K at about 12 h, at which period there is a nodal line diagonally across the resonator. Other important features of the response are resonances at 7·98 h and at 10·36 h. At 7·98 h there are two nodal lines perpendicular to the line KLM, and the maximum amplification factor of 16 is attained at K, L and M in figure 1 (b).

Alternative dimensions and the effects of the earth's rotation have been considered by Williams (1973, 1974). The rotation affects the phase of the response in the resonator, giving rise to some amphidromic points. However, the amplitude response is not very sensitive to changes of dimension or rotation, so that the response curves in figure 9 retain their significance. Currently an analysis of records from the Gulf is being undertaken, in order to determine the significance of the resonant response of the Gulf to storm surges and periodic trade winds.

The work was completed during the tenure by N. V. Williams of a C.S.I.R.O. postgraduate studentship while on leave from the Australian Department of Supply.

REFERENCES

BARTHOLOMEUZS, E. F. 1958 Reflexion of long waves at a step. *Proc. Camb. Phil. Soc.* **54**, 106–118.

JAMES, W. 1970 Resonators on narrow channels. *J. Fluid Mech.* **44**, 615–621.

JAMES, W. 1971*a* Response of rectangular resonators. *Proc. Inst. Civil Engrs*, **48**, 51–63.

JAMES, W. 1971 *b* Harbour resonators. *Proc. A.S.C.E.* **97** (WW1), 115–122.

MILES, J. W. 1947 Right angled joint in rectangular tube. *J. Acoust. Soc. Am.* **19**, 572–579.

MILES, J. W. & GILBERT, F. 1968 The scattering of gravity waves. *J. Fluid Mech.* **34**, 783–793.

MILES, J. W. & MUNK, H. W. 1961 Harbour paradox. *Proc. A.S.C.E.* **87** (WW 3), 111–130.

VALEMBOIS, J. 1953 *Proc. Minnesota Int. Hydr. Conf.*, pp. 193–200.

WILLIAMS, N. V. 1973 The application of the resonator to problems in oceanography. Ph.D. dissertation, University of New South Wales.

WILLIAMS, N. V. 1974 The gulfs of Carpentaria and Thailand. (In preparation)